Available online at www.sciencedirect.com

SciVerse ScienceDirect

Ceramics International 39 (2013) S529–S532

CERAMICS INTERNATIONAL

www.elsevier.com/locate/ceramint

Surface and optical phonon characteristics of ZnO/diamond heterostructure

S.S. Ng*, S.C. Lee, P.K. Ooi, K.G. Saw, M.J. Abdullah, Z. Hassan, H. Abu Hassan

Nano-Optoelectronics Research and Technology Laboratory, School of Physics, Universiti Sains Malaysia, Penang 11800, Malaysia

Available online 16 October 2012

Abstract

In this paper, we report on surface and optical phonon properties of ZnO/diamond heterostructure. ZnO thin film was deposited via radio-frequency magnetron sputtering on *p*-type diamond substrate. Polarized IR reflectance and attenuated total reflection (ATR) techniques were employed to investigate the optical phonon and surface phonon polariton (SPP) of the ZnO/diamond heterostructure, respectively. The obtained experimental spectra were fitted by the theoretical spectra simulated using a standard transfer matrix formulation. Overall, the experimental and theoretical spectra were in good agreement. To verify the origin of the observed ATR dip, surface polariton dispersion spectrum of the studied structure was generated based on standard multilayer reflection mapping technique. The result reveals that the detected ATR dip was attributed to the leaky SPP mode of ZnO.

Keywords: B. Spectroscopy; C. Optical properties; D. ZnO; Attenuate total reflection

1. Introduction

Nowadays, earth-abundance, inexpensive, and non-toxic zinc oxide (ZnO) is emerging as a promising material for the development of optoelectronic applications, in particular solar cells and photodetector [1]. This is mainly due to its superior physical properties, excellent optical and electrical characteristics, as well as outstanding chemical resistance profile [1–3].

However, there is one major technical issue associated with ZnO based devices. Namely, it is difficult to produce p-type ZnO semiconductor due to the self-compensating effect from native defects and/or hydrogen incorporation. For this reason, *n*-ZnO on p-type semiconductors heterojunction (i.e., *n*-ZnO/*p*-Si, *n*-ZnO/*p*-diamond, *n*-ZnO/*p*-Cu_2O, and *n*-ZnO/*p*-NiO) has been proposed [3–10]. Subsequently, the fundamental properties of these heterojunction materials have attracted a great deal of interest. Nevertheless, its surface and optical phonon characteristics have not yet been fully investigated. For instance, there is only one paper is devoted to its surface phonon polariton (SPP) characteristics [11].

Recently, the SPP characteristics have received considerable attention from the research community. This is attributed to their unique characteristics, which can be utilized for various important applications such as thermophotovoltaic energy conversion system, high density optical data storage device, and near field surface enhanced spectroscopy [12–14].

Considering the importance of fundamental physics and new potential applications of SPP, the surface and optical phonon characteristics of *n*-ZnO/*p*-diamond heterostructure will be investigated experimentally and theoretically.

2. Material and methods

Unintentional doped *n*-type ZnO thin film was deposited on the p-type (boron-doped) diamond substrate using an A500 Edwards radio frequency (RF) magnetron sputtering system at ambient temperature. A ZnO sputtering target with a diameter of 76.2 mm and purity of 99.995% was used. The ZnO thin film was deposited at an RF power of 200 W for 1 h.

Room temperature IR measurements were performed using a Fourier Transform IR (FTIR) spectrometer (Spectrum GX FT-IR, Perkin-Elmer). A wire grid thallium

*Corresponding author. Tel.: +604 6535325; fax: +604 6579150.
E-mail address: shashiong@yahoo.com (S.S. Ng).

0272-8842/$ - see front matter
http://dx.doi.org/10.1016/j.ceramint.2012.10.128

iodide bromide IR polarizer was used to obtain the polarized IR radiation.

In this work, polarized IR reflectance measurements were first carried out to access the vibrational properties of the studied structure. The IR reflectance measurements were made with a fixed angle reflectance accessory (Perkin–Elmer) at an incident angle of 16°. The spectra were recorded from 400 cm^{-1} to 7800 cm^{-1} with spectral resolution of 4 cm^{-1}. An Al-coating mirror was employed as reference standard. To investigate the SPP characteristics of the sample, *p*-polarized IR ATR measurement with Otto configuration were performed. Here, the *p*-polarized IR radiation denotes IR radiation with electric field in the plane of the incident radiation. For this measurement, an optional single-reflection diamond ATR accessory (GladiATR, PIKE Technologies) with an internal incident angle θ of 45° and a refractive index n_{prism} of 2.4 was employed. The ATR spectra were acquired in the spectral range from 400 cm^{-1} to 4000 cm^{-1} with spectral resolution of 4 cm^{-1}.

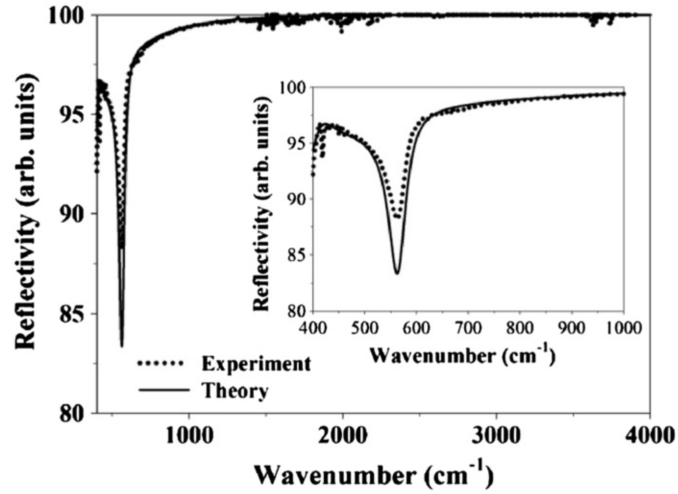

Fig. 1. Experimental and theoretical *p*-polarized IR ATR spectrum of ZnO thin film grown on *p*-diamond substrate. The inset figure is the magnification of the ATR spectrum in the range of 400–1000 cm^{-1}.

3. Theory

Let's assume that the optical *c*-axis of the ZnO crystal is parallel to the surface normal ($c_{axis}\|z$) and perpendicular to the propagation direction ($c_{axis}\perp x$). The wurtzite ZnO is optically anisotropic; two sets of phonon parameters are required to model the dielectric tensor components [15]. One set to model ε_{xx} $(\varepsilon_{yy})\equiv\varepsilon_{\perp}$ and another to model $\varepsilon_{zz}\equiv\varepsilon_{\|}$. For diamond, it is optically isotropic, $\varepsilon_{xx}=\varepsilon_{yy}=\varepsilon_{zz}\equiv\varepsilon_{\perp}$, therefore, only one set of phonon parameters is sufficient to model the dielectric tensor. By taking into account the thin film anisotropy and the contribution of free carriers, the expression for these dielectric functions can be expressed by [16]:

$$\varepsilon_j(\omega)=\left[\varepsilon_{\infty j}\left(\frac{\omega_{LOj}^2-\omega^2-i\omega\gamma_{LOj}}{\omega_{TOj}^2-\omega^2-i\omega\gamma_{TOj}}-\frac{\omega_{pj}^2}{\omega^2+i\omega\gamma_{pj}}\right)\right] \quad (1)$$

where ε_{∞} and γ are the high-frequency the dielectric constant and phonon damping, respectively. ω is the angular frequency. The subscript LO(TO) is the longitudinal-optical (transverse-optical) mode. The subscript *j* represents the parallel ($\|$) and perpendicular ($\perp$) vibrational modes with respect to the optical *c*-axis.

In this work, theoretical *p*-polarized ATR spectrum simulated using the standard transfer matrix formulation [15] was used to verify the experimental result. Theoretical surface polariton (SP) dispersion spectrum generated using the standard multilayer reflection mapping technique was used to determine the origin of the ATR feature.

4. Results and discussion

Fig. 1 shows the room temperature experimental (dotted line) and theoretical (solid line) *p*-polarized IR ATR spectra for wurtzite ZnO thin film grown on *p*-diamond substrate. One pronounced ATR dip at 562 cm^{-1} can be clearly observed. The origin of this dip is the leaky SPP mode of the ZnO thin film (will be verified later). No ATR dip corresponding to the *p*-diamond is observed because the diamond is inactive in IR region. Note that diamond is a non-polar material like silicon and germanium which does not display a net dipole moment when interacting with IR radiation.

The obtained leaky SPP mode is in reasonable agreement with the values obtained for the ZnO/SiC [17] and the ZnO/GaN/SiC [18] samples. This leaky SPP mode (as well as the leaky SPP modes of the ZnO/SiC and the ZnO/GaN/SiC samples) deviated from that obtained from the ZnO/Si sample [11]. This is mainly due to the thickness of ZnO thin film grown on Si substrate being much higher as compared to other samples. In general, the thicker ZnO thin film will tend to produce more bulk-like result. The leaky SPP mode for the ZnO/Si is about 532 cm^{-1} [11] which is closed to the real SPP mode of the bulk ZnO at 529 cm^{-1}.

In this work, the reststrahlen parameters for the studied structure were extracted from the polarized IR reflectance spectra (not shown here). The experimental spectra were fitted with the theoretical spectra generated using the standard transfer matrix formulation. Subsequently, these reststrahlen parameters were used for the simulation of the theoretical *p*-polarized ATR spectrum by using the same formulation, i.e., as shown by the solid line in Fig. 1.

Overall, it was found that the experimental and theoretical ATR spectra are in good agreement with each other. The intensity mismatches at the absorption dip (as shown in the inset of Fig. 1) is probably due to the experimental variations in the vacuum gap and incident angle [19].

Fig. 2 shows the theoretical SP dispersion spectrum of the ZnO thin film on *p*-diamond substrate simulated based on a standard three dimensional (3D) multilayer SP

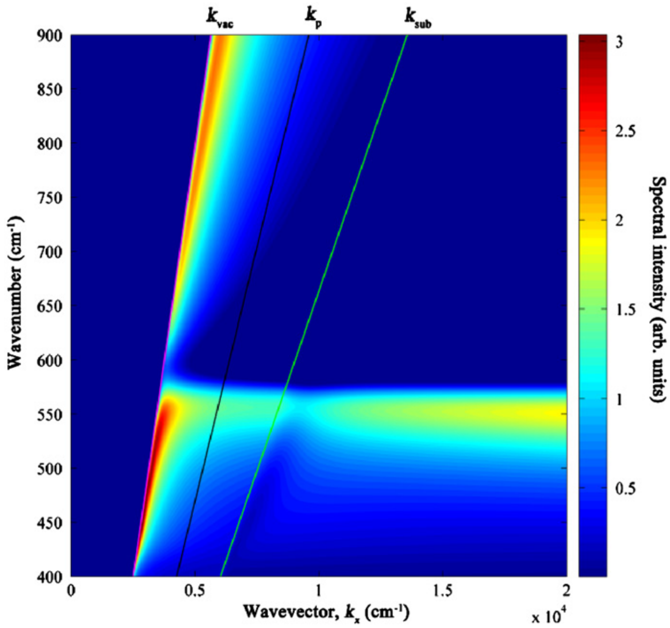

Fig. 2. Theoretical SP dispersion spectrum of wurtzite ZnO thin film grown on *p*-diamond substrate. The region with high spectral intensity corresponds to the SPP resonance of ZnO thin film. (For interpretation of the references to color in this figure legend, the reader is referred to the web version of this article.)

dispersion formulation. Also shown in Fig. 2 are the vacuum line (k_{vac}), the prism light line (k_p), and the substrate light line (k_{sub}). These lines were calculated based on $k_{vac}=(\omega/c)$, $k_p=\varepsilon^2_{diamond}(\omega/c)\sin\theta$, and $k_{sub}=(\omega/c)\varepsilon^{1/2}_{diamond}$, respectively. The symbol $\varepsilon_{diamond}$ represents the dielectric constant of diamond and c is the velocity of light in a vacuum ($3\ ms^{-1}\times 10^8\ ms^{-1}$). Note that the parameters used to model the 3D-SP dispersion spectrum are obtained from the model fit of the polarized IR reflectance spectra, as mentioned earlier.

In comparison to the conventional numerical simulation of SP dispersion curve [20], the 3D-SP dispersion spectrum has an important advantage, that is, the SPP resonance can be illustrated with least loss of information even though the damping parameters are taken into consideration. Consequently, the theoretical predictions are more comparable to the experiment with smaller discrepancy.

As seen in Fig. 2, the SP dispersion spectrum exhibits a high contrast region with relative highest spectral intensity (red–yellow–green) as compared to the background region (blue). This region corresponds to the SPP resonance of ZnO thin film, which occupies the frequency range between the TO and LO phonon frequencies of ZnO (i.e., the reststrahlen band of ZnO). The propagation of the SPP resonance strongly depends on the dielectric functions of the layered system. In general, the existence of a surface mode requires the real parts of the dielectric functions of two attached media are in opposite sign. Once the condition is satisfied then the surface mode would be localized at the interface of that attached media. In the reststrahlen band of ZnO, the real part of dielectric function of the ZnO is negative while the dielectric function of vacuum is always constant and positive (i.e., $\varepsilon_{vacuum}=1$). Therefore, the condition for the localization of SPP mode is satisfied. Subsequently, the SPP resonance propagates along the vacuum/ZnO interface and confined in the frequency range of reststrahlen band of ZnO.

From Fig. 2, it is found that the SPP resonance propagated in the wavevector region of $k_x < k_{sub}$. Subsequently, the SPP mode fell into this region and can be classified into the leaky SPP branch [18,21]. It is interesting to mention here that in conventional numerical simulation of SP dispersion curve, the leaky SPP resonance is usually inaccessible [21]. However, it can be illustrated in the 3D-SP dispersion spectrum even though the damping parameters are included.

For the ZnO/diamond interface, the localization condition of surface mode is satisfied, namely, the dielectric function of the diamond substrate is positive in the reststrahlen band of ZnO. Consequently, there should have been an interface phonon polariton (IPP) resonance propagating along the ZnO/diamond interface in the reststrahlen band of ZnO with higher wavevector ($k_x > 8000\ cm^{-1}$). However, no apparent contrast region due to the IPP resonance is observed in the SP dispersion spectrum. This phenomenon can be explained by the fact that spectral strength of this IPP resonance is relatively weak due to the damping effects of optical phonons. Namely, it is easily suppressed by phonons damping. Apart from that, this IPP resonance is also hardly to be detected practically in the ATR experiment due to the limit of instrumental capability [11,15].

In practice, the intersection of the SPP resonance in the SP dispersion spectrum with the k_p line corresponds to the ATR dip. As seen in Figs. 1 and 2, the frequency of the absorption dip in the ATR spectrum ($562\ cm^{-1}$) is in very good agreement with the result deduced from the SP dispersion spectrum ($560\ cm^{-1}$). This leads us to conclude that the detected ATR dip in Fig. 1 originated from the leaky SPP mode of the ZnO thin film. The small discrepancy is probably due to the perturbing effect of the prism during the ATR measurement, which depends on the vacuum gap between the prism base and the surface of sample [19].

5. Conclusions

In this work, the surface and optical phonon characteristics of ZnO thin film grown on *p*-diamond substrate have been investigated experimentally and theoretically. Absorption ATR dip corresponding to the leaky SPP mode of the ZnO was detected. The obtained experimental result was in good agreement with the theoretical calculation as well as the reported results.

Acknowledgements

This work was supported by the Short Term Grants (Accounts no.: 304/ PFIZIK/ 6311110 and 304/ PJJAUH/ 6311098) and Ministry of Higher Education of Malaysia

Fundamental Research Grant Scheme (Grant no.: 203/PFI-ZIK/6711197). The support of the Nano-Optoelectronics Research and Technology Laboratory, School of Physics, Universiti Sains Malaysia is gratefully acknowledged.

References

[1] U. Ozgur, Y.I. Alivov, C. Liu, A. Teke, M.A. Reshchikov, S. Dogan, V. Avrutin, S.J. Cho, H. Markoc, A comprehensive review of ZnO materials and devices, Journal of Applied Physics 98 (2005) 041301 (103# pp).

[2] V. Srikant, D.R. Clarke, On the optical band gap of zinc oxide, Journal of Applied Physics 83 (1998) 5447 (5# pp).

[3] J. Huang, L.J. Wang, K. Tang, J.J. Zhang, Y.B. Xia, X.G. Lu, The fabrication and photoresponse of ZnO/diamond film heterojunction diode, Applied Surface Science 258 (2012) 2010–2013.

[4] L. Shen, Z.Q. Ma, C. Shen, F. Li, Bo. He, F. Xu, Studies on fabrication and characterization of a ZnO/*p*-Si-based solar cell, Superlattice Microstruct 48 (2010) 426–433.

[5] W.Y. Zhang, Q.L. Meng, B.X. Lin, Z.X. Fu, Influence of growth conditions on photovoltaic effect of ZnO/Si heterojunction, Solar Energy Materials and Solar Cells 92 (2008) 949–952.

[6] S.F. Wang, M.J. Chen, X.H. Zhao, J.C. Chen, W. Yu, J.L. Wang, G.S. Fu, Photovoltaic characteristic of Al-doped ZnO/Si heterojunction, Physica B 405 (2010) 4966–4969.

[7] S. Mridha, M. Dutta, D. Basak, Photoresponse of *n*-ZnO/*p*-Si heterojunction towards ultraviolet/visible lights: thickness dependent behavior, Journal of Materials Science: Materials in Electronics 20 (2009) S376–379.

[8] H. Ohta, M. Hirano, K. Nakahara, H. Maruta, T. Tanabe, M. Kamiya, T. Kamiya, H. Hosono, Fabrication and photoresponse of a pn-heterojunction diode composed of transparent oxide semiconductors, *p*-NiO and *n*-ZnO, Applied Physics Letters 83 (2003) 1029 (3# pp).

[9] Y.I. Alivov, U. Ozgur, S. Dogan, D. Johnstone, V. Avrutin, N. Onojima, C. Liu, J. Xie, Q. Fan, H. Morkoc, Photoresponse of *n*-ZnO/*p*-SiC heterojunction diodes grown by plasma-assisted molecular-beam epitaxy, Applied Physics Letters 86 (2005) 241108 (3# pp).

[10] K.G. Saw, S.S. Tneh, F.K. Yam, S.S. Ng, Z. Hassan, Ultraviolet photoresponse properties of zinc oxide on type IIb diamond heterojunction, Physica B 405 (2010) 4123–4127.

[11] S.S. Ng, O.H. Ooi, S.C. Lee, M.J. Abdullah, Z. Hassan, H. Abu Hassan, Surface phonon polariton characteristics of wurtzite ZnO thin film grown on silicon substrate, Physica Status Solidi B 249 (2012) 1058–1062.

[12] N. Ocelic, R. Hillenbrand, Subwavelength-scale tailoring of surface phonon polaritons by focused ion-beam implementation, Nature Materials 3 (2004) 606–609.

[13] A.J. Huber, N. Ocelic, D. Kazantsev, R. Hillenbrand, Near-field imaging of mid-infrared surface phonon polariton propagation, Applied Physics Letters 87 (2005) 081103 (3# pp).

[14] M. Francoeur, M.P. Menguc, R. Vaillon, Local density of electromagnetic states within a nanometric gap formed between two thin films supporting surface phonon polaritons, Journal of Applied Physics 107 (2010) 034313 (8# pp).

[15] T. Dumelow, T.J. Barker, S.R.P. Smith, D.R. Tilley, Far-infrared spectroscopy of phonons and plasmons in semiconductor superlattices, Surface Science Reports 17 (1993) 151–212.

[16] F. Gervais, B. Piriou, Anharmonicity in several-polar-mode crystals: adjusting phonon self-energy of LO and TO modes in Al_2O_3 and TiO_2 to fit infrared reflectivity, Journal of Physics C: Solid State Physics 7 (1974) 2374–2386.

[17] S.C. Lee, S.S. Ng, N.H. Al-Hardan, M.J. Abdullah, Z. Hassan, H. Abu Hassan, Studies of surface and interface phonon polariton characteristics of wurtzite ZnO thin film on wurtzite 6H-SiC substrate by *p*-polarized infrared attenuated total reflection spectroscopy, Thin Solid Films 519 (2011) 3703–3708.

[18] S.C. Lee, S.S. Ng, P.K. Ooi, Z. Hassan, H. Abu Hassan, N.H. Al-Hardan, M.J. Abdullah, V.A. Yakovlev, N.N. Novikova, Surface and interface phonon polariton characteristics of wurtzite ZnO/GaN heterostructure, Applied Physics Letters 98 (2011) 241909 (3 pages).

[19] A.A. Hamilton, T. Dumelow, T.J. Parker, S.R.P. Smith, Far infrared attenuated total reflection spectroscopy for investigating superlattice phonon parameters, Journal of Physics: Condensed Matter 8 (1996) 8027–8040.

[20] S.C. Lee, S.S. Ng, P.K. Ooi, Z. Hassan, H. Abu Hassan, Dispersion of surface and interface phonon polariton modes in wurtzite based multilayer system, Journal of the Physical Society of Japan 80 (2011) 084712 (7# pp).

[21] T. Dumelow, A.R. El Gohary, K.A. Maslin, T.J. Parker, D.R. Tilley, S.N. Ershov, Analysis of far infrared spectra showing bulk and surface phonon polaritons in CdTe epilayers on GaAs substrates, Physica Status Solidi B 161 (1990) 233–244.